

Multi-chiral doublets in one single nucleus

J. Meng,^{1, 2, 3,*} J. Peng,¹ S. Q. Zhang,¹ and S.-G. Zhou^{2, 3}

¹*School of Physics, Peking University, Beijing 100871*

²*Institute of Theoretical Physics, Chinese Academy of Science, Beijing 100080*

³*Center of Theoretical Nuclear Physics, National Laboratory of Heavy Ion Accelerator, Lanzhou 730000*

Abstract

Adiabatic and configuration-fixed constraint triaxial relativistic mean field (RMF) approaches are developed for the first time and a new phenomenon, the existence of multi-chiral doublets ($M\chi D$), i.e., more than one pairs of chiral doublets bands in one single nucleus, is suggested for ^{106}Rh based on the triaxial deformations together with their corresponding proton and neutron configurations.

PACS numbers: 21.10.Re, 21.60.Jz, 21.10.Pc, 21.10.Gv, 27.60.+j

*e-mail: mengj@pku.edu.cn

The handedness or chirality is a subject of general interests in molecular physics, elementary particles, and optical physics. The occurrence of chirality in nuclear physics was suggested in 1997 [1] and the predicted patterns of spectra exhibiting chirality, i.e., the chiral doublets bands, were experimentally observed in 2001 [2].

Since the pioneer work on chirality in nuclear physics, lots of efforts have been made to understand the new phenomena and explore their possible existence in the nuclear chart, e.g., [3, 4, 5, 6, 7, 8, 9, 10]. Experimentally, the chiral doublets bands have been identified in many nuclei in $A \sim 130$ mass region with the earlier suggested configuration $\pi h_{11/2} \otimes \nu h_{11/2}^{-1}$, $A \sim 100$ with $\pi g_{9/2}^{-1} \otimes \nu h_{11/2}$, and $A \sim 190$ with $\pi h_{9/2} \otimes \nu i_{13/2}^{-1}$. On theoretical aspect, the chiral symmetry breaking was firstly predicted in the particle-rotor model (PRM) and tilted axis cranking (TAC) approach for triaxially deformed nuclei [1]. It has been investigated later in hybrid Woods-Saxon and Nilsson model combined with shell correction method [7] as well as the Skyrme-Hartree-Fock cranking approach [8], and its selection rules for electromagnetic transitions have been discussed in a simple PRM [9].

For triaxially deformed rotational nucleus, the collective angular momentum favors alignment with the intermediate axis, which in this case has the largest moment of inertia. Meanwhile, the valence particle and hole angular momentum vectors align along the nuclear short and long axis, respectively. These orientations maximize the overlap of the particle densities with the triaxial core and minimize the interaction energy. The three mutually perpendicular angular momenta can be arranged to form two systems with opposite chirality, a left- and a right-handedness. They are transformed into each other by the chiral operator which combines time reversal and spacial rotation of 180° , $\chi = \mathcal{T}\mathcal{R}(\pi)$. The breaking of the chiral symmetry in atomic nucleus is observed due to the quantum tunnelling between the systems with opposite chirality.

The description for the quantum tunnelling of the chiral partners is beyond the mean field, as the usual cranking approach is a semiclassical model and the total angular momentum is not a good quantum number [11]. In contrast, the PRM is better suited for this purpose, which however is so far confined for one particle and one hole configurations only [1, 9, 10]. Its generalization for more particles and/or holes are still under development. Furthermore the deformation γ and configurations in PRM are not self-consistent rather as inputs of the model.

The relativistic mean field (RMF) theory has received wide attention due to its success in

describing the properties of nuclei and many nuclear phenomena for the past years [12, 13]. It is interesting to search for nuclei with triaxial deformation and configurations with not only one particle and one hole but also multi-particle and multi-hole suitable for chirality in RMF theory. A multi-dimensional microscopic cranking RMF model is very time consuming and has only been applied in magnetic rotation so far [14].

In this Letter, we will develop the adiabatic and configuration-fixed constraint triaxial RMF approaches to investigate the triaxial shape coexistence and the possible chiral doublets bands in $A \sim 100$ mass region. The existence of multi-chiral doublets ($M\chi D$), i.e., more than one pairs of chiral doublets bands in one single nucleus, will be suggested via the examining the deformation and the corresponding configurations.

In RMF theory, the nuclei are characterized by an attractive scalar field $S(\mathbf{r})$ and a repulsive vector field $V(\mathbf{r})$ in the Dirac equation,

$$\{-i\boldsymbol{\alpha} \cdot \nabla + V(\mathbf{r}) + \beta[M + S(\mathbf{r})]\}\psi_i = \varepsilon_i \psi_i, \quad (1)$$

which can be solved by expanding separately the upper and lower components of the spinor ψ_i in terms of eigenfunctions of the three-dimensional deformed oscillator in Cartesian coordinates $\phi_\alpha(\mathbf{r})$ and its time reversal state $\phi_{\bar{\alpha}}(\mathbf{r}) = \hat{T}\phi_\alpha(\mathbf{r})$ with $\hat{T} = i\hat{\sigma}_y K$,

$$\psi_i(\mathbf{r}) = \begin{pmatrix} \sum_\alpha f_\alpha^{(i)} \phi_\alpha(\mathbf{r}) \\ \sum_{\bar{\alpha}} i g_{\bar{\alpha}}^{(i)} \phi_{\bar{\alpha}}(\mathbf{r}) \end{pmatrix}. \quad (2)$$

In order to avoid the complex matrix diagonalization problem in Ref. [15], $\phi_\alpha(\mathbf{r})$ is written as a product of three Hermite polynomials [16],

$$\phi_\alpha(\mathbf{r}) = \frac{i^{n_y}}{\sqrt{2}} \phi_{n_x}(x) \phi_{n_y}(y) \phi_{n_z}(z) \begin{pmatrix} 1 \\ (-1)^{n_x+1} \end{pmatrix}. \quad (3)$$

The meson fields are expanded similarly with the same deformation β_0 and γ_0 for the basis, but an oscillator length smaller by a factor of $\sqrt{2}$ than that for the nucleons ($b_B = b_0/\sqrt{2}$) has been used in order to simplify the calculations and to avoid the necessity of additional parameters. The oscillator frequency is $\hbar\omega_0 = 41A^{-1/3}$ MeV.

In order to check the convergence of the results with the number of expanded oscillator shells for fermions n_{of} , the binding energies (upper) and the deformations β (middle) and

γ (lower) calculated with effective interaction PK1 [17] for ^{106}Rh as functions of n_{of} are presented in Fig. 1. The legends (filled circles, open circles, squares, triangle ups, triangle downs, and diamonds) represent the results obtained in basis with different deformation ($\beta_0 = 0.0, 0.1, 0.2, 0.3, 0.4$ and 0.5 , respectively). It shows that as long as $n_{\text{of}} \geq 10$, the binding energies as well as the deformations β and γ obtained are almost the same. Furthermore they are independent on the deformation β_0 of the basis. Similar convergence check for the bosons has also been done. In the following, a spherical basis with 12 major oscillator shells for fermions and 10 shells for bosons will be used, which gives an error less than 0.1% for the binding energy.

In general the triaxial RMF calculation leads to only some local minima. In order to get the ground state for triaxial deformed nucleus, constraint calculations are necessary and in principle such calculations should be carried out in two-dimensional β and γ plane. As such two-dimensional constraint calculations turn out to be expensive even for modern computer facilities, therefore the constraint calculations with $\langle \hat{Q}_{20}^2 + 2\hat{Q}_{22}^2 \rangle$, i.e., β^2 , are carried out to search for the ground state for triaxially deformed nucleus.

The energy surface and the deformation γ as functions of deformation β in adiabatic constraint triaxial RMF calculation with PK1 for ^{106}Rh are presented as open circles in Fig. 2(a) and (b) respectively. There are some irregularities in the energy surface. Furthermore some local minima are too obscure to be recognized and it is technically difficult to understand their corresponding single particle configurations. We therefore performed the configuration-fixed constraint calculation similar to what have been done in the non-relativistic case [18]. Starting from any point in the energy surface in the adiabatic constraint calculations, the configuration-fixed constraint calculation requires that the single particle orbits occupied are fixed during the constraint calculation, i.e.,

$$|\langle \psi_j(\beta + \delta\beta) | \psi_i(\beta) \rangle| \approx 1. \quad (4)$$

The energy surfaces and the deformations γ in configuration-fixed calculations with PK1 for ^{106}Rh are given as solid lines in Fig. 2(a) and (b) respectively. For each fixed configuration, the constraint calculation gives a continuous and smooth curve for the energy surface and the deformation γ as a function of deformation β . The irregularities in the adiabatic energy surface disappear. In comparison, the minima in the energy surfaces of the configuration-fixed constraint calculations become obvious, which are respectively represented by stars

and labelled as A, B, C, D, E, F and G. Their corresponding deformations β and γ together with their binding energies are respectively given in Fig. 2(a) and (b). It is interesting to note that, for each fixed configuration, the deformation γ is approximately a constant (as in Fig 2(b)), which means that the deformation γ is mainly determined by its corresponding configuration.

The energies for these minima including the ground state are within 1.3 MeV to each other but correspond to different deformations β and γ , which is a good example of the shape coexistence. The shape coexistence here is different from the spherical, oblate and prolate shape coexistence, e.g., in neutron-deficient Pt, Hg and Pb isotopes. It is the triaxial shape coexistence, i.e., for the ground state A: the binding energy $E = 903.92$ MeV (the data 906.72 MeV), deformation $\beta = 0.27$ and $\gamma = 24.7^\circ$, the excited minima B: $E = 903.82$ MeV, $\beta = 0.25$ and $\gamma = 23.3^\circ$, C: $E = 903.28$ MeV, $\beta = 0.30$ and $\gamma = 22.9^\circ$, and D: $E = 902.69$ MeV, $\beta = 0.22$, $\gamma = 30.8^\circ$. All the states A, B, C, and D have deformation β and γ suitable for chirality [1, 10]. As these states are all in one single nucleus, if chiral doublets bands can be built on these states, it may lead to a new phenomenon, the existence of $M\chi D$ in one single nucleus. Therefore, in the following, we will investigate their proton and neutron configurations in detail to see whether the particle and hole configurations required by chirality are available.

Performing the configuration-fixed constraint calculations for the ground state, the single particle levels can be obtained as functions of deformation β . The difference in single particle levels obtained by choosing other minima is negligible. The neutron and proton single particle levels obtained in such a way are presented in Fig. 3. The positive (negative) parity states are marked by solid (dashed) lines and the occupations corresponding to the minima in Fig. 2 are represented by filled circles (two particles) and stars (one particle). The corresponding quantum numbers for spherical case are labelled at the left side of the levels. As the energy curves become very stiff for small deformation in Fig. 2, the present configuration-fixed constraint calculations cannot be performed for deformation $\beta < 0.06$. Therefore we cannot distinguish the occupation of some low- j orbits, e.g., the last occupied neutron orbit for state A may come from $2d_{5/2}$ or $2d_{3/2}$, as marked in the figures. However, as the nuclear chirality is essentially determined by the high- j orbits, such illegibility does not influence the conclusions here.

The binding energies, deformations β and γ as well as the corresponding configurations

extracted from Fig. 3 for the minima A, B, C, and D in ^{106}Rh obtained in the configuration-fixed constraint triaxial RMF calculations with PK1 are listed in Table. I. Except the state D, in which there is no high- j neutron valence particle, we found the high- j proton and neutron configuration for the ground state (state A) as $\pi(1g_{9/2})^{-3} \otimes \nu(1h_{11/2})^2$, state B as $\pi(1g_{9/2})^{-3} \otimes \nu(1h_{11/2})^1$, and state C as $\pi(1g_{9/2})^{-3} \otimes \nu(1h_{11/2})^3$, respectively. All of them have high- j proton holes and high- j neutron particles configurations, which together with their triaxial deformations favor the construction of the chiral doublets bands. It is interesting to note that the states A and B compete strongly with each other in energy. However, due to different parities, the states A and B do not mix up and are possible to produce the new phenomenon M χ D. So far, a pair of chiral doublets bands with negative parity have been observed in ^{106}Rh [5]. It will be interesting to search for other chiral doublets bands in this nucleus.

Similar to ^{106}Rh , detailed constraint calculations are also performed for other isotopes in $A \sim 100$ mass region and the possibilities of M χ D exist in other nuclei as well. The results will be published elsewhere in details. Here in Fig. 4, the deformations β and γ for ground states in $^{98-114}\text{Rh}$, $^{102-116}\text{Ag}$ and $^{100-118}\text{In}$ isotopes are presented. The shaded area represents the favorable deformation γ for nuclear chirality. The nuclei, ^{104}Rh and ^{106}Rh , in which the chiral doublets bands have been observed [4, 5], are marked as filled circles. Apart from ^{104}Rh and ^{106}Rh , the favorable deformation γ for chirality has been found in $^{102,108,110}\text{Rh}$, $^{108-112}\text{Ag}$ and ^{112}In , which implicates that more chiral doublets bands can be expected in $A \sim 100$ mass region. For each isotope chain, the deformation γ varies with the neutron number due to different occupation in $\nu h_{11/2}$.

In summary, adiabatic and configuration-fixed constraint triaxial RMF approaches are developed for the first time to investigate the triaxial shape coexistence and possible chiral doublets bands. A new phenomenon, the existence of multi-chiral doublets (M χ D), i.e., more than one pairs of chiral doublets bands in one single nucleus, is suggested in ^{106}Rh by examining the deformation and the corresponding configurations. Similar investigations have also been done for Rh, Ag and In isotopes and also with other effective interactions. The observation of M χ D is very promising in this mass region.

This work is partly supported by the Major State Basic Research Development Program Under Contract Number G2000077407, the National Natural Science Foundation of China

under Grant No. 10435010, 10221003, and 10475003, the Doctoral Program Foundation from the Ministry of Education in China, and the Knowledge Innovation Project of Chinese Academy of Sciences under contract Number KJCX2-SW-N02.

- [1] S. Frauendorf and J. Meng, Nucl.Phys. **A617**,131(1997).
- [2] K. Starosta, *et al.*, Phys. Rev. Lett. **86**, 971 (2001).
- [3] D. L. Balabanski, *et al.*, Phys. Rev. C **70**, 044305 (2004).
- [4] C. Vaman, *et al.*, Phys. Rev. Lett. **92**, 032501 (2004).
- [5] P. Joshi, *et al.* Phys. Lett. B **595**, 135 (2004).
- [6] J. Timár, *et al.* Phys. Lett. B **598**, 178 (2004).
- [7] V. Dimitrov, *et al.*, Phys. Rev. Lett. **84**, 5732 (2000).
- [8] P. Olbratowski, *et al.*, Phys. Rev. Lett. **93**, 052501(2004).
- [9] T. Koike, *et al.*, Phys. Rev. Lett. **93**, 172502(2004).
- [10] J. Peng, *et al.*, Phys. Rev. C **68**, 044324 (2003).
- [11] S. Frauendorf, Rev. Mod. Phys. **73**, 463 (2001).
- [12] P. Ring, Prog. Part. Nucl. Phys. **37**, 193 (1996).
- [13] J. Meng, Nucl. Phys. **A635**, 3 (1998).
- [14] H. Madokoro, *et al.*, Phys. Rev. C **62**, 061301(R) (2000).
- [15] D. Hirata, *et al.*, Nucl. Phys. **A609**, 131 (1996).
- [16] W. Koepf and P. Ring, Nucl. Phys. **A493**, 61 (1989).
- [17] W. H. Long, *et al.*, Phys. Rev. C **69**, 034319 (2004).
- [18] L. Guo, *et al.*, Nucl. Phys. **A740**, 59 (2004).

TABLE I: The binding energies, deformations β and γ and the corresponding configurations for the minima A, B, C, and D in ^{106}Rh obtained in the configuration-fixed constraint triaxial RMF calculations with PK1.

| State | E (MeV) | β | γ | Configurations |
|-------|----------|---------|----------|---|
| A | 903.9150 | 0.270 | 24.7° | $\pi(1g_{9/2})^{-3} \otimes \nu \{(1h_{11/2})^2[(2d_{5/2})^1 \text{ or } (2d_{3/2})^1]\}$ |
| B | 903.8196 | 0.246 | 23.3° | $\pi(1g_{9/2})^{-3} \otimes \nu \{(1h_{11/2})^1[(2d_{5/2})^2 \text{ or } (2d_{3/2})^2]\}$ |
| C | 903.2790 | 0.295 | 22.9° | $\pi(1g_{9/2})^{-3} \otimes \nu(1h_{11/2})^3$ |
| D | 902.6960 | 0.215 | 30.8° | $\pi(1g_{9/2})^{-3} \otimes \nu[(2d_{5/2})^3 \text{ or } (2d_{3/2})^3]$ |

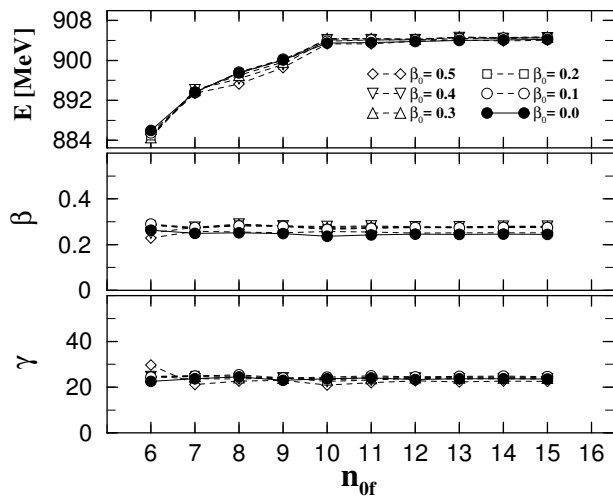


FIG. 1: Total binding energy, deformation β and γ calculated with PK1 for ^{106}Rh as functions of the number of expanded oscillator shells for fermions n_{of} . The filled circles, open circles, squares, triangle ups, triangle downs, and diamonds represent the results as the deformation of basis β_0 equals to 0.0, 0.1, 0.2, 0.3, 0.4 and 0.5, respectively.

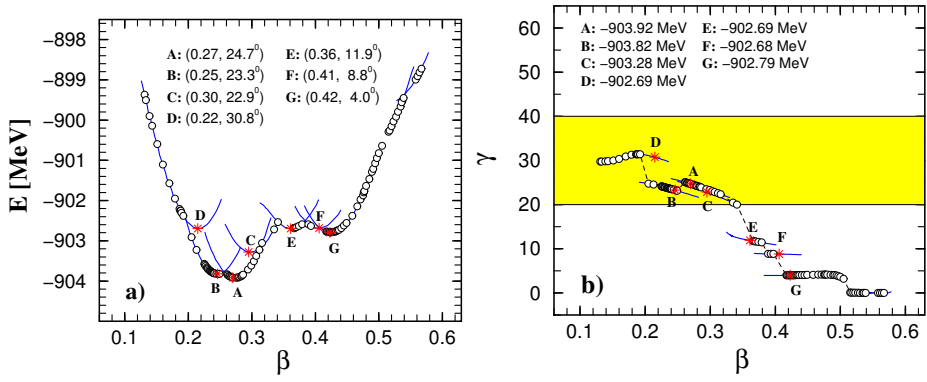


FIG. 2: (color online) The energy surfaces (a) and the deformations γ (b) as functions of deformation β in adiabatic (open circles) and configuration-fixed (solid lines) constraint triaxial RMF calculation with PK1 for ^{106}Rh . The minima in the energy surfaces are represented as stars and labelled respectively as A, B, C, D, E, F and G. Their corresponding deformations β and γ together with their energies are respectively given in (a) and (b).

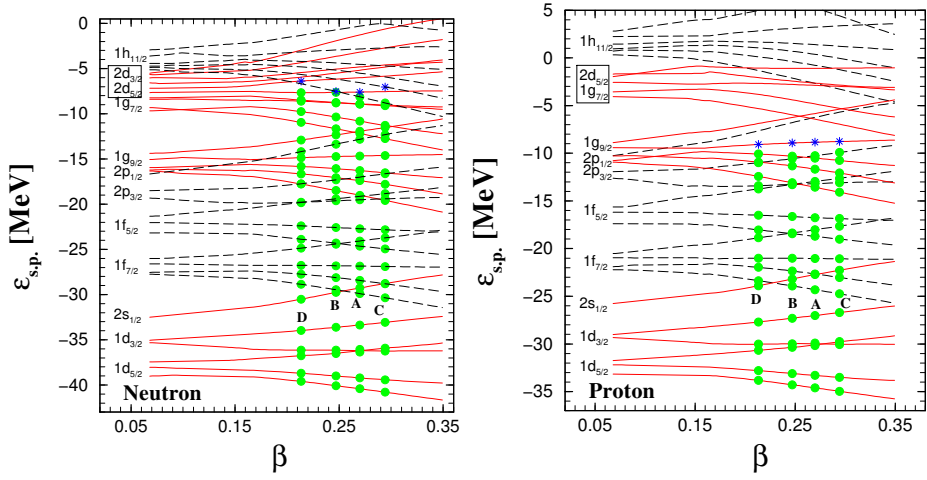


FIG. 3: (color online) The neutron and proton single particle levels obtained in configuration-fixed constraint triaxial RMF calculations with PK1 for ^{106}Rh as functions of the deformation β . Positive (negative) parity states are marked by solid (dashed) lines. The occupations corresponding to the minima in Fig. 2 are represented by filled circles (two particles) and stars (one particle).

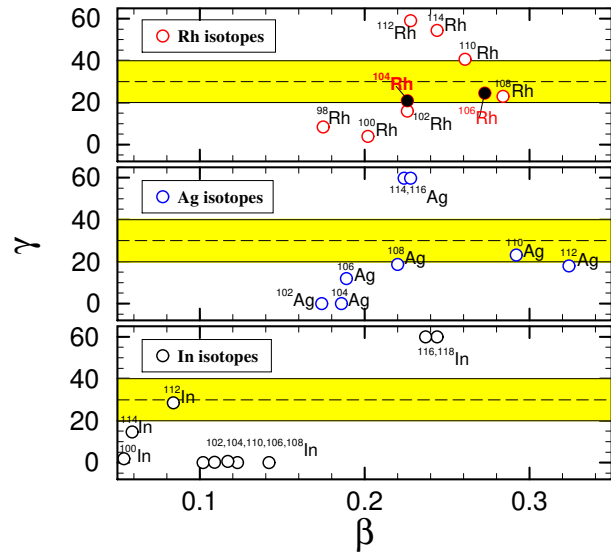


FIG. 4: (color online) The deformations β and γ for the ground states in Rh (upper), Ag (middle) and In (lower) isotopes in constraint triaxial RMF calculations with PK1. The shaded area represents the favorable deformation γ for nuclear chirality. The nuclei ^{104}Rh and ^{106}Rh , in which the chiral doublets bands have been observed, are marked as filled circles.